INNOVATION FOREVER
Open Access

Innovation Discovery

ISSN 2959-5150 (Online)

Short Communication

Theoretical, Spectral Characterization and Cytotoxicity Assessment of Newly Synthesized Cerium(III) Complex

Irena Kostova[1*], Vasile Chiş[2], Jan Mojžiš[3]

[1]*Department of Chemistry, Faculty of Pharmacy, Medical University, Sofia, Bulgaria*
[2]*Department of Biomedical Physics, Faculty of Physics, Babeş-Bolyai University, Cluj-Napoca, Romania*
[3]*Department of Pharmacology, Faculty of Medicine, P.J. Šafarik University, Košice, Slovakia*

[*]***Correspondence to: Irena Kostova, PhD, DSc, Professor,*** *Department of Chemistry, Faculty of Pharmacy, Medical University-Sofia, 2 Dunav St., Sofia 1000, Bulgaria; E-mail: irenakostova@yahoo.com*

Abstract

Uracil derivatives are promising ligands for the synthesis of metal coordination compounds with diverse biological activities, including anticancer effects. Among these, lanthanide(III) complexes are of particular interest in medicinal chemistry. This work describes the synthesis, theoretical, analytical and spectral characterization of cerium(III) (Ce(III)) complex of orotic acid (HOA). The FT-IR and FT-Raman analysis completed for the compounds, orotic acid, its Na salt and Ce(III) complex, facilitated elucidating the vibrational performance of the vibrational modes of the ligand, sensitive to coordination with metal ions. The antiproliferative activity of the tested compounds has been determined using MTT dye-reduction assay. Comprehensive vibrational analysis of orotic acid, its Na salt and Ce(III) complex supported by the theoretical and experimental spectra confirmed the binding modes in the newly synthesized Ce(III) complex. Substantial alterations in the IR and Raman spectra of Ce(III) complex have been detected in comparison to the vibrational spectra of the ligand and its sodium salt, confirming the proposed metal-ligand modes. The theoretical wavenumbers including vibrational scattering activities have been found in good agreement with the recorded vibrational spectra. The investigated compounds have been screened for their *in-vitro* cytotoxicity against tumour cells in order to prove their biological activity. Screening revealed that the studied compounds exhibited cytotoxic effects on the evaluated tumor cells.

Keywords: cerium(III) complex, orotic acid, FT-IR, Raman, cytotoxicity evaluation

Received: November 2, 2025
Revised: December 16, 2025
Accepted: December 29, 2025
Published: December 31, 2025

Citation: Kostova I, Chiş V, Mojžiš J. Theoretical, Spectral Characterization and Cytotoxicity Assessment of Newly Synthesized Cerium(III) Complex. *Innov Discov*, 2025; 2(4): 20.

1 INTRODUCTION

Lanthanide(III) (Ln(III)) coordination compounds are of significant interest due to their wide range of biological applications. The unique characteristics of Ln ions, including their large ionic radii and coordination numbers, present both challenges and opportunities for constructing complexes with novel structures and distinctive properties. Achieving control over the shapes and dimensions of these complexes relies heavily on the choice of suitable organic ligands as well as the synthetic strategies employed. Recently, we have reported thorough studies on the optimized geometries and vibrational characterization of different Ln(III)-based model systems of bioactive ligands to suggest the metal–ligand binding mode by using high-level theoretical methods[1-4]. Ligands that contain both nitrogen and oxygen donor atoms exhibit flexible coordination behavior, making them especially valuable in the formation of diverse coordination frameworks. For this reason, Ln(III) complexes formed with biologically active derivatives of orotic acid merit thorough investigation.

The biologically active ligand orotic acid (2,6-dioxo-1,2,3,6-tetrahydropyrimidine-4-carboxylic acid, vitamin B_{13}, HOA, Figure 1A) and its coordination chemistry has been an area of great interest[5], ranging from bioinorganic to pharmaceutical and materials chemistry. Metal orotates are widely applied in medicine[6]. Many orotate derivatives have been screened as therapeutic agents for cancer[7].

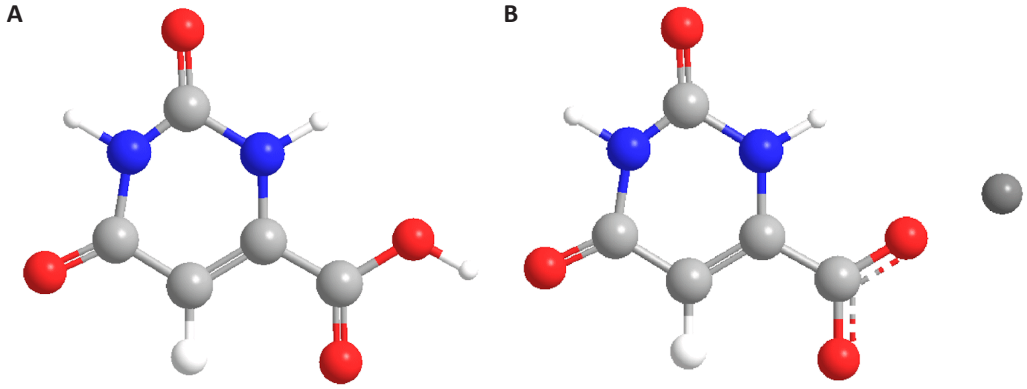

Figure 1. The Structures of Orotic Acid (A) and Orotic Acid Sodium Salt (B).

The structural formula of Na salt of the ligand (NaOA) is shown in Figure 1B. More recent interest has focused on the proposed biological function of orotic acid and its corresponding anions for metal ions, which is held responsible for the successful application of orotate complexes in curing syndromes associated with a deficiency of biogenic metals[8].

Orotic acid acts as a diacid in water solution. The multifunctionality of its anions offers interesting possibilities in crystal engineering as a versatile ligand for supramolecular assemblies[9]. The coordinated orotates display a ligand surface with double or triple H-bonding abilities, dependent on the coordination, and have therefore a possibility to adopt several modes of inter-ligand H-bonding to form extended self-assembled buildings. However, earlier studies on the coordination of orotic acid and its derivatives primarily focused on d-block or alkali metal cations, while Ln have been neglected. Orotic acid displays versatile coordination modes, making the synthesis of new Ln(III) complexes challenging, particularly for anticancer applications. To date, Ln(III) complexes with orotic acid and reported cytotoxic activity have not been described. We have recently synthesized lanthanide complexes with a number of biologically active ligands, and we reported their significant cytotoxic activity in different human cell lines as well as their antioxidant activity[10-18]. Motivated by the promising findings, we sought to develop new Ln complexes of this ligand. The reason to synthesize new complexes of biologically active uracils was to compare and find out the differences between known and the newly obtained Ln(III) complexes with bioactive ligands. This study aimed to synthesize and characterize a cerium(III) (Ce(III))-orotic acid complex to investigate its cytotoxic properties.

In this work we report theoretical and spectral results on the Ce(III) complex of orotic acid (HOA). The Ce(III)-OA binding was characterized by elemental analysis, FTIR and FTRaman spectroscopies. For assessment of the reactive sites for electrophilic attack of the ligand and binding with the metal, DFT calculations of the structures of HOA, sodium salt of orotic acid NaOA and Ce(III)–OA model systems have been performed.

Since the newly obtained Ce(III) complex of orotic acid (HOA) does not possess a crystalline structure and such data were not available, theoretical approaches for determination of the geometrical parameters, vibrational frequencies, hydrogen bond strengths, and the binding mode for the model Ln(III)–ligand at a high level of theory are very helpful for extracting reliable structural information as shown in our previous work[1-4,14-18]. The methodology employed was found to be robust for the series of Ln complexes, yielding results consistent with those reported in the literature. The cytotoxicity of both the ligand and Ce(III) complex was assessed using the MTT assay across multiple tumor cells.

2 MATERIALS AND METHODS

2.1 Synthesis of the Complex

All compounds used in the preparation of the solutions were purchased from Merck, p.a. grade: $Ce(NO_3)_3.6H_2O$. The Na salt of the ligand was used for the syntesis of Ce(III) complex.

The complex was prepared by interaction of Ce(III) nitrate and the Na salt of the ligand in water solution, in metal:ligand molar ratio of 1:2. The complex formation can be presented by the equations:

$$NaOA+H_2O \leftrightarrow Na^+ + OH^- + HOA \quad (1)$$

$$[Ce(H_2O)_n]^{3+} + H_2O \leftrightarrow [Ce(OH)(H_2O)_{n-1}]^{2+} + H_3O^+ \quad (2)$$

$$[Ce(OH)(H_2O)_{n-1}]^{2+} + 2OA^- \rightarrow Ce(OA^-)_2(OH)(H_2O) + (n-3)H_2O, \quad (3)$$

where $HOA = C_5N_2O_4H_4$ and $OA^- = C_5N_2O_4H_3^-$.

The complex was obtained by adding a water solution of Ce(III) salt to a water solution of Na salt of the ligand stirring at room temperature for one hour. At mixing of the solutions, we obtained the light-yellow precipitate which was filtered (pH 5.0), washed with water and dried to constant mass. The yield of the complex after drying was 88%. The complex exhibited poor solubility in water and common alcohols, but dissolved well in DMSO.

2.2 Chemistry Device Descriptions

The C, H and N contents were determined by elemental analysis. The content of water was determined by Karl Fisher and thermogravimetrical analyses.

The FTIR of the ligand and Ce(III) complex were recorded in KBr in the 4000-400cm^{-1} frequency range by FT-IR 113V Bruker spectrometer.

The Raman spectra of the compounds were recorded with a Dilor Labram spectrometer (Horiba-Jobin-Yvon, model LabRam) using the 784.8nm excitation line from a near infrared Diode laser. The Labram integrated system is coupled trough an Olympus LMPlanFL 50x objective to the optical microscope. The spectra were collected in the backscattering geometry with a resolution of 2cm^{-1}. The detection of Raman signal was carried out with a Peltier-cooled CCD camera. The laser power of 35mW was used in our measurements.

2.3 Computational Details

The geometry of orotic acid and its Ce(III) complex were optimized using the Gaussian 03 program[19]. Becke's three-parameter exchange functional (B3)[20] with Perdew and Wang's gradient-corrected correlation functional (PW91)[21,22] and Becke's three-parameter hybrid exchange functional (B3)[23,24] using the LYP correlational functional of Lee, Yang and Parr (LYP)[25] were employed in the DFT calculations. The 6-311++G** Pople split valence basis sets along with the LANL2DZ basis set implemented in the Gaussian 03 program[19] were chosen in the geometry optimization and normal modes calculations. The LANL2DZ basis set[26] was chosen with the intention to optimize the new Ce(III) complex of the orotic acid because of the atomic number of cerium.

Density functional theory (DFT) calculations of harmonic vibrational modes were performed on the fully optimized molecular geometries. Analytical computations of harmonic vibrational wavenumbers, including IR and Raman intensities, were carried out for these structures. The observation of only real vibrational wavenumbers confirms that all optimized geometries correspond to true global minima on the potential energy surfaces.

2.4 Tumour Cell Lines

Jurkat (human T-cell acute lymphoblastic leukemia), HeLa (human cervical adenocarcinoma) MCF-7 (human breast adenocarcinoma, estrogen receptor-positive), MDA-MB-231 (human breast adenocarcinoma, estrogen receptor-negative) and A-549 (human lung adenocarcinoma) cells were obtained from Dr. M. Hajdúch (Olomouc, Czech Republic) and the CCRF-CEM cell line (human T-cell acute lymphoblastic leukemia) - from the German Collection of Microorganisms and Cell Cultures (Braunschweig, Germany).

The cells were routinely maintained in RPMI 1640 medium with L-Glutamine and HEPES (Jurkat, HeLa and CCR-CEM) or Dulbecco's modified Eagle's medium with Glutamax-I (MCF-7, MDA-MB-231, and A-549) supplemented with 10% fetal calf serum, penicillin (100IU/ mL) and streptomycin (100μg/mL) (all from Invitrogen, USA), in humidified air with 5% CO_2 at 37°C. Before each cytotoxicity assay, cell viability was determined by trypan blue exclusion method and found greater than 95%.

2.5 Cytotoxicity Assay

The cytotoxic effects of orotic acid, sodium salt of orotic acid and Ce(III) complex were determined using colorimetric microculture assay with the MTT end-point[27]. Briefly, 3×10^3 (A-549, MCF-7, MDA-MB-231), 5×10^3 (HeLa) or 1×10^4 (Jurkat and CEM) cells were plated per well in 96-well polystyrene microplates (Sarstedt, Germany) in the culture medium containing tested chemicals at final concentrations of 10^{-4}-10^{-9}mol/L. After 72h of incubation, 10μL of MTT (5mg/mL) (Sigma, Germany) were added in each well. After an additional 4h, during which insoluble formazan was produced, 100μL of 10% sodium dodecylsulphate were added in each well and another 12h were allowed for the dissolution of formazan. Absorbance was measured at 540nm using the automated MRX microplate reader (Dynatech Laboratories, UK). The blank-corrected absorbance of the control wells was taken as 100% and the results were expressed as a percentage of the control. All experiments were performed in triplicate.

3 RESULTS AND DISCUSSION

3.1 Chemistry

The composition of the Ce(III) complex was determined by elemental analysis. The metal content was obtained after mineralization. The content of water was determined thermogravimetrically and by Karl Fisher analysis. FTIR and FTRaman spectra confirmed the structure of the complex.

Elemental analysis of Ce(III) complex: (% calculated/found): $Ce(OA)_2(OH).3H_2O$: C: 23,03/23.53; H: 2,49/2.71; N: 10,75/10,52; H_2O: 10,36/10,34; Ce: 26,87/26,50, where HOA = $C_5N_2O_4H_4$ and OA^- = $C_5N_2O_4H_3^-$.

The bonding mode of the ligand to Ce(III) cations was determined by comparing the IR and Raman spectra of the complex and the ligand as well as with the theoretical calculations. The vibrational fundamentals from the IR and Raman spectra were analysed by comparing these modes with those from the literature[28-35] in combination with the results of our DFT calculations (i.e., harmonic vibrational wavenumbers and their Raman scattering

Table 1. Selected Calculated Structural Parameters of Ce(III) Complex of Orotic Acid at the B3LYP/cc-pVDZ(SDD) Level of Theory

Dihedral Angles (°)				**Calculated Value**
C5	C6	N1	C2	-0.2
C4	C5	C6	N1	0.1
N3	C2	N1	C6	0.1
H5	C5	C6	N1	180.0
O2	C2	N3	C4	180.0
O4	C4	C5	C6	-180.0
H3	N3	C2	O2	0.0
H1	N1	C2	O2	0.0
C7	C6	N1	C2	179.7
O1	C7	C6	N1	-0.3
O3	C7	C6	N1	179.7
C2'	O1	C7	C6	149.8
N1'	C2'	O1	C7	-148.5
C6'	N1'	C2'	O1	-83.8
C5'	C6'	N1'	C2'	-0.1
C4'	C5'	C6'	N1'	0.0
N3'	C2'	O1	C7	110.9
H5'	C5'	C6'	N1'	180.0
O2'	C2'	O1	C7	-57.4
O4'	C4'	C5'	C6'	-179.9
H3'	N3'	C2'	O1	-168.3
H1'	N1'	C2'	O1	96.1
C7'	C6'	N1'	C2'	179.9
O3'	C7'	C6'	N1'	0.3
O1'	C7'	C6'	N1'	-179.7
Ce	O1	C7	C6	-2.3
O5	Ce	O1	C7	2.8
H6	O5	Ce	O1	-5.8
Ce–O Distances				**Calculated Value (Å)**
Ce–O1				2.156
Ce–O5				2.062

activities) for the ligand[34] and for the Ce(III) complex.

3.2 Geometry Optimization

The calculated structural parameters of orotic acid have been published by Kostova et al[34]. Because no crystal structure data were available for Ce(III) complex of orotic acid, its structure was optimized at different levels of theory (B3PW91/6-311++G**, B3PW91/LANL2DZ, B3LYP/6-311++G**, B3LYP/LANL2DZ, B3LYP/cc-pVDZ(SDD)) and compared with literature data for compounds containing identical or similar functional groups[34]. The B3LYP/cc-pVDZ(SDD) theoretical level was found to be the most reliable.

The calculated parameters of Ce(III) complex of orotic acid are presenrted in Table 1 with the respective labelling of atoms, shown under the table. Orotic acid structure has been calculated and previous published data[34] helped us to get better inside.

The Ce(III) cation is at least three-coordinate, bonded to the carboxylate oxygen atoms of two orotate ligands and to a hydroxide ion. The complex is mononuclear, with each metal center coordinated by two orotate ligands and one hydroxide ion.

3.3 Vibrational Spectral Data

In Table 2 the theoretical and experimental FTIR and FTRaman data with their assignment are listed. The vibrational spectra of HOA, NaOA and Ce(III)–OA are shown in Figures 2 and 3. The vibrational fundamentals from the IR and Raman spectra were analyzed by comparing these modes with those from the literature[34] in combination with the results of our DFT calculations (i.e., harmonic vibrational wavenumbers and their Raman scattering activities).

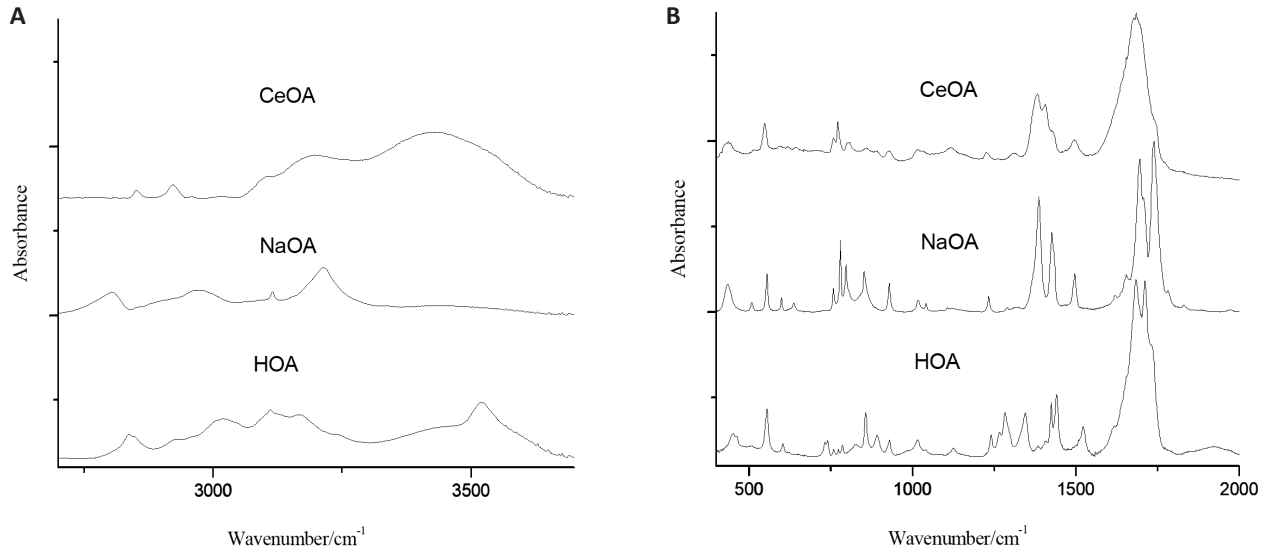

Figure 2. IR Spectra of HOA, NaOA and Ce(III) Complex. A: 2700-3700cm^{-1}; B: 400-2000cm^{-1}.

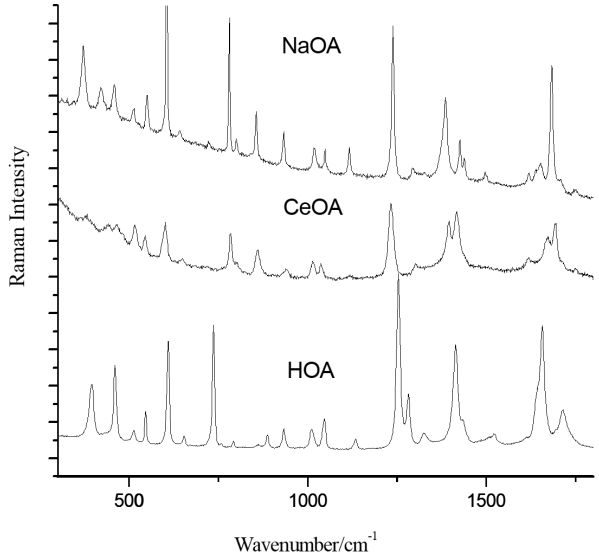

Figure 3. Raman Spectra of HOA, NaOA and Ce(III) Complex. Excitation: 784.8 nm, 35 mW.

In the IR spectral region 3600-2000cm^{-1} the O-H and N-H stretching vibrations give rise to IR bands with medium intensity (Figure 2A). The assignment of the O-H and N-H bands is quite difficult (Figure 2A) is quite difficult because they appear overlapped in the same spectral region, and the involvement of these groups in hydrogen bonds affects their wavenumbers and produces a relevant band broadening[29,31-35]. The medium IR bands at 3520cm^{-1} (HOA) and 3437cm^{-1} (Ce(III) complex) were attributed to the N-H stretches, whereas the shoulder at 3232cm^{-1} (HOA) and the medium band at 3199cm^{-1} (Ce(III)) were assigned to the O-H stretching vibrations (Table 2). The wavenumber region 2700-2500cm^{-1} in the IR spectra of the orotic acid and its complex is typical of strongly hydrogen bonded intermolecular complexes with overtones and combinations of lower frequency modes of the bonded molecules[36-43].

For hydrogen-bonded, non-dimerized carbonyls, a mode active in both IR and Raman appears at 1730–1705cm^{-1}. In our IR spectra, a strong band at 1712cm^{-1} (orotic acid) was assigned to the symmetrical C2=O2 stretch and the N–H stretch. In this region were observed one medium band at 1715cm^{-1} in the Raman spectrum of the free ligand, and two shoulders at 1748 and 1714cm^{-1} in the Raman spectrum of the complex (Figure 2B)[36-40]. In the IR spectra, the strong bands at 1684cm^{-1} for orotic acid and 1682cm^{-1} for its Ce(III) complex were assigned to the symmetrical stretching of C4=O4 and the C6=C5 bond. Corresponding Raman bands appear at 1657cm^{-1} and 1676cm^{-1}, respectively.

In the IR spectrum, the asymmetrical COO^- stretching mode appears at 1522cm^{-1} for orotic acid and as a shoulder at 1604cm^{-1} for its Ce(III) complex, while the symmetrical mode is observed at 1407cm^{-1} and 1380cm^{-1}, respectively. In the Raman spectra, the symmetrical COO^- stretch appears as a strong peak at 1414cm^{-1} for the free ligand and a medium-strong band at 1392cm^{-1} for the complex (Figures 2B and 3).

In the 1800–900cm^{-1} IR region, bands at 1424cm^{-1}for the ligand and 1410cm^{-1} for the complex are assigned to N–H stretching. These vibrations are notably shifted and differ in intensity in the Raman spectra for the ligand and its complex.

The C5–H5, N1–H1, and C–O–H bending modes are observed in both IR and Raman spectra. For the free ligand, they appear at 1284cm^{-1} in IR and 1282cm^{-1}in Raman, shifting to 1308cm^{-1} and 1300 cm^{-1}, respectively, upon coordination with Ce(III). A weak band at 1266cm^{-1}, seen only in the IR spectrum of orotic acid, is attributed to the C=O bending mode and the symmetrical stretching of N1–C2–N3. Another weak peak at 1241cm^{-1}, present only in the free ligand's IR spectrum, corresponds to the stretching of C2–N3–C4 and C6=C5–C4; in Raman spectra, these vibrations are also observed for the

Table 2. Selected Theoretical (B3LYP/cc-pVDZ(SDD) and Experimental IR and Raman Wavenumbers (cm^{-1}) of Orotic Acid (HOA) and Its Ce(III) Complex (CeOA) and Their Tentative Assignment

Nr	Sym	Freq. [cm^{-1}]	Freq. Scaled	IR Intensity	IR [%]	Raman Activity	Raman Intensity [%]	Exp. Raman		Exp. IR		Assignments
								HOA	CeOA	HOA	CeOA	
1	A	2.56	3	2.518	0.21	0.7613	0.00					δ(O1-Ce-O1')[13.7%], δ(O1-Ce-O3')[12.4%], τ(C7-O1-Ce-O3') [11.1%]
2	A	9.9809	10	1.8178	0.15	0.9773	0.00					δ(O1-Ce-C7')[8.5%] δ(O3'-Ce-O5)[8.4%] δ(C7'-Ce-O1')[6.4%]
3	A	20.4761	20	0.6633	0.06	8.9026	0.00					τ(C7-O1-Ce-O1')[20.2%], τ(C7-O1-Ce-O5)[19.4%]
4	A	26.6238	27	3.1672	0.26	3.8755	0.00					τ(C6-C7-O1-Ce[11.4%], δ(O3'-Ce-O5)[9.0%]
5	A	50.531	51	0.9239	0.08	0.5284	0.00					δ(C7-O1-Ce)[11.5%]
6	A	61.5319	62	1.8111	0.15	0.5581	0.00					γ(O1-Ce)[8.1%]
7	A	65.8648	66	1.2715	0.11	0.7931	0.00					γ(O1-Ce)[26.5%], γ(C7-O1)[21.9%]
8	A	86.5911	87	0.2961	0.02	0.1153	0.00					γ(O1-Ce)[45.0%], γ(C7-O1)[23.6%]
9	A	97.3053	97	0.1894	0.02	0.3292	0.00					τ(C7-O_2)[16.4%]+τ(C7'-O_2)[15.8%]
10	A	99.984	100	3.0449	0.25	1.5927	0.00					τ(C7-O_2)[22.7%], γ(O5-Ce)[11.4%]
11	A	128.7094	129	2.6957	0.22	1.5771	0.24					γ(C2'-N3')[9.7%], γ(N1'-C2'[8.5%], +δ(O1-Ce-O5) [4.2%]
12	A	132.3557	132	7.5654	0.63	0.534	0.08					γ(O1-Ce)[10.1%]
13	A	135.4941	135	5.4077	0.45	1.5408	0.23					δ(O1-Ce)[5.7%]
14	A	158.9358	159	20.6932	1.72	0.227	0.03					δ(O1-Ce-O5)[12.6%]
15	A	160.6485	161	8.8252	0.73	0.424	0.06					γ(C4'-N3')[12.5%]
16	A	162.7356	163	0.5491	0.05	0.2461	0.04					γ(O1-Ce)[26.8%], γ(C7-O1)[13.3%]
17	A	185.3578	185	17.2045	1.43	0.8196	0.12					γ(C2-N1)[8.1%], γ(C2-N3)[6.9%]
18	A	185.7174	186	18.47	1.54	0.4224	0.06					γ(C2-N1)[7.5%], γ(C2 – N3)[6.5%]
19	A	188.3407	188	2.7435	0.23	0.8398	0.13					γ(C2' – N1')[10.6%], γ(C5'-N4')[9.3%]
20	A	253.3862	253	95.791	7.96	5.3575	0.81		306			ν(O1-Ce)[11.6%]
21	A	268.9943	269	14.8812	1.24	0.369	0.06					ν(O1'-Ce)[12.9%], ν(O3'-Ce)[12.2%]
22	A	337.3602	337	1.1089	0.09	2.8636	0.43		345			ν(C6-C7)[7.0%]
23	A	379.7051	380	7.1679	0.60	2.3258	0.35	395	373			ν(O1'-Ce)[8.8%] ν(C7'-Ce)[7.8%] ν(O3'-Ce)[7.5%] δ(C5'-C4'-O4')[7.3%] δ(N3'-C2'-O2')[6.3%] δ(N1'-C2'-O2')[6.2%] δ(N3'-C4'-O4')[6.0%]
24	A	409.4275	409	76.4458	6.35	0.8133	0.12					δ(C5-C4-O4)[6.6%], γ(O5-H6)[5.5%], δ(C2-N3-C4)[4.9%], δ(N1-C2-O2)[4.7%]
25	A	434.0877	434	227.8777	18.94	3.4138	0.52		440		434	ν(O1'-Ce)[10.1%], ν(O3'-Ce)[8.0%], ν(C7'-Ce)[7.6%]
26	A	454.6701	455	6.1872	0.51	1.897	0.29					γ(O5-H6)[13.0%], ν(O3'-Ce)[7.9%], ν(O1'-Ce)[5.7%], δ(C6'-C7'-O1') [4.9%], δ(C6'-C7'-O3')[4.9%],
27	A	463.7959	464	5.1374	3.91	1.8421	0.28	460	460	451		δ(C6-C7-O1)[5.7%], ν(O1-Ce)[5.7%], δ(C7-O1-Ce)[5.5%], δ(N1-C2-O2)[3.7%]

https://doi.org/10.53964/id.2025020

28	A	469.9193	470	53.6589	4.46	3.0021	0.46					γ(O5-H6)[22.4%], γ(N1-H1)[12.2%]
29	A	480.2551	480	335.9156	27.92	5.2433	0.80					γ(O5-H6)[32.0%], γ(H1-O5)[6.1%]
30	A	505.696	506	43.2524	3.59	2.6344	0.40	513	519	507	517	γ(C7-O1)[11.9%], γ(N1-C6)[9.9%], γ(C6-C7)[9.7%]
31	A	509.7985	510	17.6465	1.47	1.2924	0.20					γ(C6′-C7′)[14.5%], δ(N1′-C6′-C5′)[10.0%]
32	A	528.7598	529	17.3825	1.44	3.5874	0.54					δ(C5′-C4′-N3′)[7.0%], δ(N3′-C4′-O4′)[6.8%], δ(C6′-C5′-C4′)[6.4%], δ(C2′-N1′-C6′)[6.2%] δ(N3′-C2′-O2′)[5.4%], δ(N1′-C2′-N3′)[5.3%], δ(C2′-N3′-H3′)[5.0%]
33	A	533.3859	533	8.7439	0.73	10.9407	1.66	546	553	555	549	γ(HI-O5)[7.2%], δ(N3-C4-O4)[5.5%], δ(C6-C5-C4)[5.3%], δ(C5-C4-N3)[5.3%], δ(C2-N1-C6)[5.1%]
34	A	579.2959	579	5.1137	0.43	13.2429	2.01					δ(C2-N3-C4)[6.7%], γ(C4-N3)[5.7%], δ(N1-C2-N3)[5.2%]
35	A	581.7457	582	29.2636	2.43	9.8861	1.50					δ(C2′-N3′-C4′)[5.5%], γ(C4′-N3′)[5.0%]
36	A	595.7573	596	154.5158	12.84	12.7471	1.93	608	608	603	595	ν(Ce-O5)[21.4%]
37	A	614.8493	615	23.7935	1.98	1.9047	0.29					γ(N1′-H1′)[57.1%]
38	A	630.7345	631	0.9089	0.08	1.6572	0.25					δ(N1′-C2′-O2′)[7.3%], δ(C5′-C4′-O4′)[6.1%], δ(N3′-C4′-O4′)[5.6%], δ(N1′-C6′-C7′)[5.2%], δ (C6′-C7′-O3′)[5.1%]
39	A	637.0082	637	4.1856	0.35	1.9524	0.30					δ(N1-C2-O2)[7.2%], δ(C5-C4-O4)[6.6%], δ(C6-C7-O1)[5.9%], δ(N3-C4-O4)[5.7%], δ(N1-C6-C7)[5.6%], δ(N3-C2-O2)[5.3%]
40	A	659.3762	659	1.8011	0.15	2.2342	0.34					δ(N3-C2-N1)[9.1%], γ(N3-H3)[8.0%], γ(H1-N1)[8.0%]
41	A	690.5054	691	72.5632	6.03	3.907	0.59	653	643		645	γ(N3′-H3′)[56.3%], γ(N1′-H1′)[15.0%]
42	A	695.8344	696	77.9368	28.47	3.5934	0.55					γ(N3-H3) [18.2%], δ(N1-C2-N2)[11.0%], γ(N1-H1)[9.2%]
43	A	742.8497	743	7.0132	0.58	1.1305	0.17					γ(C2′-N1′) [17.2%], γ(C4′-N3′) [7.7%]
44	A	757.8471	758	6.134	0.51	1.2531	0.19					γ(O2-C2) [8.5%], γ(H5-C5)[8.3%]
45	A	765.2464	765	42.0068	3.49	0.0786	0.02	753	757	758		γ(C2′O) [12.8%], γ(C2′N) [10.7%]
46	A	768.6012	769	58.7518	4.88	0.1456	0.04					γ(C2-O2) [22.0%], γ(C2N) [11.6%]
47	A	782.1262	782	45.1071	3.75	4.7131	0.72					δ(C7O_2)[8.4%], ν(O1-Ce)[6.6%]
48	A	795.3514	795	113.7463	9.45	14.8325	4.58	792	787	786	772	δ(C7′O_2)[8.1%], ν(C7′-Ce)[5.4%]
49	A	799.9312	800	53.5037	4.45	1.3874	0.43					γ(O1-Ce) [24.8%], w(CO_2)[15.9%], γ(C-H, N-H)[14.1%]
50	A	809.9882	810	40.2118	3.34	0.3116	0.10					w(CO_2)[20.0%], γ(C-H)[11.9%]
51	A	885.3006	885	12.6743	1.05	3.8833	1.20	887	874	892		γ(C5′-H5′)[14.6%], γ(C5′-C4′)[13.9%], γ(C6′-C5′)[10.0%], γ(C4′-N3′)[10.0%]
52	A	890.8805	891	14.5007	1.21	3.2354	1.00					γ(C5-H5)[43.9%]
53	A	929.8159	930	20.8788	1.74	2.0722	0.64	933	939	930	926	ν(C6′-C7′)[4.8%]
54	A	931.3051	931	13.3944	1.11	2.4026	0.74					ν(C6-C7)[5.4%], δ(C2-N3-C4)[1.5%]
55	A	1001.8738	963	10.0139	0.83	7.6455	2.36					δ(C2′-N3′-H3′)[8.7%], δ(C4′-N3′-H3′)[6.8%], δ(C4′-C5′–H5′)[6.2%], δ(C2′-N1′-H1′)[5.6%], δ(C6′-C5′-H5′)[5.1%]
56	A	1012.0876	973	28.5922	2.38	13.979	4.32	1011	1016	1015	1014	δ(C2-N3-H3)[7.3%], δ(C2-N3-H3)[6.7%], δ(C6-C5-H5)[5.9%], δ(C2-N1-C6)[5.8%]

https://doi.org/10.53964/id.2025020

57	A	1022.0397	983	103.3644	8.59	4.325	1.34					v(C6-C7)[6.4%], δ(C6-C5-C4)[5.8%], δ(N1-C6-C5)[5.1%], δ(C4-C5-H5)[5.0%]
58	A	1031.6341	992	17.9826	1.49	2.2655	0.70	1047	1047	1042		δ(C6′-C5′-C4′)[6.5%], δ(N1′-C6′-C5′)[6.3%], v(C6′-C7′)[5.8%], δ(C2′-N1′-C6′)[5.8%]
59	A	1113.8593	1071	28.4689	2.37	4.225	1.30		1119			δ(C4′-C5′-H5′)[11.2%], δ(C6′-C5′-H5′)[10.8%]
60	A	1117.7298	1075	31.3739	2.61	4.4717	1.38	1134	1145	1125	1114	δ(C6-C5-H5)[10.7%], δ(C4-C5-H5)[10.4%]
61	A	1212.1927	1165	20.8327	1.73	12.6067	3.89		1205			v(C4-N3)[10.8%]
62	A	1215.6927	1169	28.2751	2.35	15.1272	4.67	1254	1244	1241		v(C4′-N3′)[10.1%]
63	A	1251.8475	1204	1203.1367	100.00	17.1773	5.30					v(C7-O1)[12.7%]
64	A	1297.4308	1247	3.8982	0.32	4.0174	1.24	1282	1300	1284	1308	δ(N1′-H1′)[23.0%], δ(C5′-H5′)[22.3%]
65	A	1332.713	1281	273.7719	22.75	19.2546	5.95	1326	1318	1345		δ(N1-H1)[10.2%], δ(C5-H5)[10.0%]
66	A	1388.2394	1335	1.9042	0.16	14.3108	4.42					δ(N3-H3)[50.2%]
67	A	1395.5705	1342	7.5453	0.63	16.8251	5.20					δ(N3′-H3′)[45.9%]
68	A	1396.7491	1343	143.2046	11.90	4.0191	1.24					v(C2′-N3′)[8.8%], v(C2′-N1′)[8.0%], v(C4′-N3′)[5.7%]
69	A	1428.1847	1373	178.9714	14.88	0.1002	0.03					v(C2-N1)[8.6%], v(C2-N3)[7.6%]
70	A	1438.9372	1383	740.2409	61.53	119.0813	36.77	1414	1392	1407	1380	v_s(C7′O_2)[15.1%],v(C6′-C7′)[9.2%]
71	A	1523.2264	1464	306.6704	25.49	29.0754	8.98	1522		1522	1604	v(N1′-C6′)[9.6%], v(C7′-O3′)[6.7%], v(C6′-C7′)[6.0%]
72	A	1532.8515	1474	78.6414	6.54	9.5157	2.94					δ(N1H)[29.8%], v(C6-N1)[10.9%]
73	A	1573.1006	1512	131.4062	10.92	38.3153	11.83					v_{as}(C7′-O_2)[12.8%]
74	A	1677.1187	1612	20.2184	1.68	114.8285	35.46	1615	1619	1617	1641	v(C6-C5)[16.0%]
75	A	1688.0753	1623	3.161	0.26	232.6078	71.83					v(C6′-C5′)[14.9%]
76	A	1789.6134	1721	1088.913	90.51	79.0993	24.43	1657	1676	1684	1682	v(C4-O4)[10.4%]
77	A	1794.3698	1725	396.3087	32.94	174.6081	53.92					v(C4′-O4′)[12.9%]
78	A	1796.432	1727	167.53	13.92	12.8178	3.96		1748			v(C7-O3)[11.5%]
79	A	1806.2149	1736	418.3757	34.77	26.7172	8.25	1715	1714	1712		v(C2-O2)[14.9%]
80	A	1836.5128	1766	657.0465	54.61	14.3076	4.42					v(C2′-O2′)[18.1%]
81	A	3261.6657	3136	7.4902	0.62	68.0154	21.00					v(C5-H5)[74.8%]
82	A	3264.1053	3138	7.8708	0.65	53.8649	16.63					v(C5′-H5′)[75.1%]
83	A	3488.5166	3354	658.9156	54.77	323.8112	100.00			3520	3437	v(N1-H1)[44.7%], v(H1-O5)[40.3%]
84	A	3584.6337	3446	86.7059	7.21	132.4454	40.90					v(N3′-H3′)[77.2%]
85	A	3588.524	3450	70.4206	5.85	125.3322	38.71					v(N3-H3)[77.8%]
86	A	3600.0661	3461	138.1924	11.49	76.4385	23.61					v(N1′-H1′)[76.9%]
87	A	3788.1235	3642	231.2059	19.22	167.2932	51.66	3144		3232	3199	v(O5-H6)[87.3%]

https://doi.org/10.53964/id.2025020

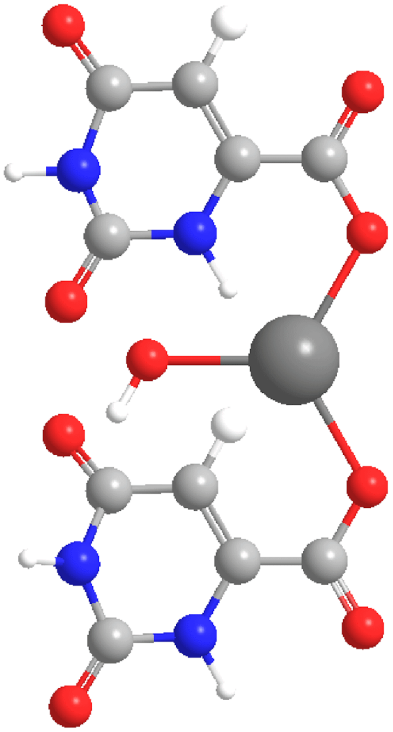

Figure 4. The Structure of Ce(III) Complex of HOA.

complex and appear as very strong bands at 1254 cm^{-1} (orotic acid) and 1232 cm^{-1} (Ce(III) complex, Figure 3).

Bands near 1015 cm^{-1}, weak in IR and medium in Raman, are assigned to the symmetrical C=O stretching mode, while those around 930 cm^{-1}, also weak in IR and medium in Raman, correspond to the symmetrical C(ring)–C(carboxyl) bridge bond stretching.

The uracilate ring bending vibrations and skeletal deformation bands of free orotic acid, mainly in the 900–300cm^{-1} region, exhibit significant changes upon complex formation (Figures 2B and 3; Table 2). These variations are likely due to distortions of the uracilate rings induced by coordination.

In the Ce(III) complex, a new band appears at 434cm^{-1} in the IR spectrum and at 440cm^{-1} in the Raman spectrum, which can be attributed to cerium–oxygen interactions[29,30,35]. Additionally, in the low-wavenumber region of the Raman spectrum, the medium-intensity band at 395cm^{-1} in free orotic acid shifts to 373cm^{-1}in the Ce(III) complex and decreases in intensity. This one and the new neighbouring band at 345cm^{-1} (in the Raman spectrum of the complex) can be due to the cerium-oxygen vibration modes[44-48]. The metal cation affects the carboxylate and the ring structure. The ionic potential of the metal is the most important parameter responsible for the influence of the metal on the rest of the molecule[49-51]. The carboxylic acids interact with the metals as symmetric[52,53] bidentate carboxylate anions and both oxygen atoms of the carboxylate are symmetrically bonded to the metal[54]. In this sense, we can observe in the Raman spectra of the Ce(III) complex a very weak peak at 306cm^{-1}, which can be due to the O-Ce-O vibration modes (Table 2)[48,55-57].

In conclusion, the present study underscores the remarkable versatility of the orotate ligand, which exhibits multiple coordination modes. The ligand's charge and coordination behavior exert a profound influence on the supramolecular architecture of the resulting complexes. Combined with previous findings, our results demonstrate that the intrinsic properties of orotic acid make its various anionic forms highly adaptable ligands for a wide spectrum of metals. This adaptability enables diverse coordination geometries, the formation of high-nuclearity aggregates, and the construction of extended polymeric networks. These features position orotic acid as a powerful and broadly applicable polyfunctional ligand, offering significant appeal to coordination chemists.

Based on detailed vibrational analysis, the most plausible structure of the synthesized Ce(III) complex has been proposed (Figure 4).

3.4 Pharmacology

The data of the preliminary cytotoxicity screening of orotic acid, its Na salt and Ce(III) complex are given in Table 3. The studied compounds were tested for the cytotoxicity on the Jurkat (human T-cell acute lymphoblastic leukemia), HeLa (human cervical adenocarcinoma) MCF-7 (human breast adenocarcinoma, estrogen receptor-positive), MDA-MB-231 (human breast adenocarcinoma, estrogen receptor-negative) and A-549 (human lung adenocarcinoma) cell lines. The results indicated that the compounds exerted moderate cytotoxicity upon the teste cells. In CCRF-CEM and A-549 cell lines, the complex's activity was very similar to or even slightly worse than the activity of NaOA. Despite the moderate cytotoxicity of the studied complex, these results can shed light on the biological profiles of lanthanides and are useful for comparative purposes.

4 CONCLUSION

The Ce(III) complex of orotic acid was synthesized and characterized by elemental analysis and vibrational spectroscopy (IR and Raman). Comparative vibrational studies of orotic acid and the Ce(III) complex revealed ligand vibrational modes sensitive to metal coordination. The results indicate that orotic acid coordinates in a monodentate manner through the carboxylic oxygen atoms of both ligands, along with one hydroxide ion, elucidating the most probable metal–ligand binding mode.

Preliminary cytotoxicity screening of the investigated compounds revealed antiproliferative activity for the Ce(III) complex, consistent with our earlier findings on lanthanide coordination compounds with bioactive ligands.

Table 3. Cytotoxicity of studied compounds at a concentration 10^{-4} mol/L (% of living cells compared to control (100%)

Compound	Cancer Cell Lines					
	Jurkat	CCRF-CEM	HeLa	A-549	MCF	MDA
OA	63.3	61.2	84.7	96.9	93.9	93.76
NaOA	58.6	64.8	78.6	90.6	100.0	93.7
CeOA	60.3	70.4	77.2	90.8	82.6	90.9

In many cases, complex formation has been shown to enhance efficacy of the lanthanide complexes. Ce(III) complex of orotic acid exerted moderate cytotoxic activity against the tested cell lines. Thus, it necessitates further more detailed pharmacological evaluation.

Acknowledgments

The administrative support received by the European Union-Next Generation EU, through the National Recovery and Resilience Plan of the Republic of Bulgaria, project No. BG-RRP-2.004-0004-C01 is greatly acknowledged.

Conflicts of Interest

All authors declared no conflict of interest.

Data Availability

All data generated or analyzed during this study are included in this published article.

Author Contribution

Kostova I conceptualized and supervised the study; Kostova I and Mojžiš J collected the experimental data; Chiş V peformed the software; Kostova I, Chiş V, and Mojžiš J analysed and investigated the data; Kostova I preparated the original draft, reviewed and edited the manuscript.

Abbreviation List

Ce(III), Cerium(III)
CeOA, Cerium complex of orotic acid
DFT, Density functional theory
DMSO, Dimethyl sulfoxide
HOA, Orotic acid
Ln(III), Lanthanide(III)
MTT, 3-[4,5-dimethylthiazol-2-yl]-2,5 diphenyl tetrazolium bromide
NaOA, Sodium salt of orotic acid

References

[1] Safronov NE, Kostova I, Palafox MA et al. Combined NMR Spectroscopy and Quantum-Chemical Calculations in Fluorescent 1,2,3-Triazole-4-carboxylic Acids Fine Structures Analysis. *Int J Mol Sci*, 2023; 24: 8947.[DOI]

[2] Yadav RK, Yadav RA, Kostova I. Experimental IR, Raman, and UV-Vis Spectra DFT Structural and Conformational Studies: Bioactivity and Solvent Effect on Molecular Properties of Methyl-Eugenol. *Molecules*, 2023; 28: 5409.[DOI]

[3] Palafox MA, Belskaya NP, Kostova I. Study of the Molecular Architectures of 2-(4-Chlorophenyl)-5-(pyrrolidin-1-yl)-2H-1,2,3-triazole-4-carboxylic Acid Using Their Vibrational Spectra, Quantum Chemical Calculations and Molecular Docking with MMP-2 Receptor. *Pharmaceutics*, 2023; 15: 2686.[DOI]

[4] Palafox MA, Todorov L, Belskaya NP et al. The Spectroscopic Characterization and Photophysical Properties of a Hydrated Lanthanum Ion Complex with a Triazole Ligand by Several DFT Methods. *Molecules*, 2025; 30: 3412.[DOI]

[5] Yurdakul Ö, Köse DA. Importance of electron donating properties of orotic acid in coordination chemistry. *J Mol Struct*, 2025; 142660.[DOI]

[6] Marynowicz W, Borski N, Flis Z et al. Orotic acid induces apoptotic death in ovarian adult granulosa tumour cells and increases mitochondrial activity in normal ovarian granulosa cells. *Reproduct Biol*, 2023; 23: 100790.[DOI]

[7] Anwar MM, Meseguer S, García-Rodríguez N et al. NK-A 17E-233I: a novel competitive inhibitor of human dihydroorotate dehydrogenase (DHODH) for cancer therapy. *J Exper Clin Cancer Res*, 2025; 44: 292.[DOI]

[8] Liu Y, Wang Y, Song S et al. Cancer therapeutic strategies based on metal ions. *Chem Sci*, 2021; 12: 12234-12247.[DOI]

[9] Lin B, Liu Y, Wang M et al. Intermolecular interactions and solubility behavior of multicomponent crystal forms of orotic acid: prediction and experiments. *Cryst Growth Des*, 2021; 21: 1473-1481.[DOI]

[10] Todorov L, Traykova M, Saso L et al. In Vitro Interaction of 5-Aminoorotic Acid and Its Gallium (III) Complex with Superoxide Radical, Generated by Two Model Systems. *Int J Mol Sci*, 2020; 21: 8862.[DOI]

[11] Todorov L, Saso L, Benarous K et al. Synthesis, Structure and Impact of 5-Aminoorotic Acid and Its Complexes with Lanthanum(III) and Gallium(III) on the Activity of Xanthine Oxidase. *Molecules*, 2021; 26: 4503.[DOI]

[12] Kostova I, Mojžiš J, Chiş V. Theoretical and Experimental Vibrational Characterization of Biologically Active Nd(III) Complex. *Molecules*, 2021; 26: 2726.[DOI]

[13] Todorov L, Kostova I. Recent Trends in the Development of Novel Metal-Based Antineoplastic Drugs. *Molecules*, 2023; 28: 1959.[DOI]

[14] Palafox MA, Belskaya NP, Kostova I. Peculiarities of the Spatial and Electronic Structure of 2-Aryl-1,2,3-Triazol-5-Carboxylic Acids and Their Salts on the Basis of Spectral Studies and DFT Calculations. *Int J Mol Sci*, 2023; 24: 14001.[DOI]

[15] Palafox MA, Belskaya NP, Todorov L et al. Structural Study of a La(III) Complex of a 1,2,3-Triazole Ligand with Antioxidant Activity. *Antioxidants*, 2023; 12: 1872.[DOI]

[16] Joe H, Atanasova V, Mojžiš J et al. Synthesis, Characterization, and Cytotoxicity of a Ga (III) Complex with Warfarin. *Inorganics*, 2024; 12: 177.[DOI]

[17] Palafox MA, Belskaya NP, Todorov L et al. Effect of Lanthanide Ions and Triazole Ligands on the Molecular Properties, Spectroscopy and Pharmacological Activity. *Int J Mol Sci*, 2024; 25: 7964.[DOI]

[18] Palafox MA, Belskaya NP, Todorov L et al. The Spectroscopic

Characterization and Photophysical Properties of a Hydrated Lanthanum Ion Complex with a Triazole Ligand by Several DFT Methods. *Front Chem*, 2024; 12: 1450106.[DOI]

[19] Frisch MJ, Trucks GW, Schlegel HB et al. Gaussian 03, Revision B. 04. Gaussian Inc, Pittsburgh, PA, USA; 2003.

[20] Becke AD. Density-functional thermochemistry. III. The role of exact exchange. *J Chem Phys*, 1993; 98: 5648-5652.[DOI]

[21] Perdew JP. Electronic Structure of Solids. Akademie Verlag, Berlin, Germany; 1991: 11.

[22] Perdew JP, Wang Y. Accurate and simple analytic representation of the electron-gas correlation energy. *Phys Rev B*, 1992; 45: 13244.[DOI]

[23] Becke AD. Density-functional thermochemistry. II. The effect of the Perdew–Wang generalized-gradient correlation correction. *J Chem Phys*, 1992; 97: 9173-9177.[DOI]

[24] Gelfand LS, Iaconianni FJ, Pytlewski LL et al. Nicotinic and isonicotinic acid n-oxide interactions with 3d metal perchlorates. *J Inorg Nucl Chem*, 1980; 42: 377-385.[DOI]

[25] Lee C, Yang W, Parr RG. Development of the Colle-Salvetti correlation-energy formula into a functional of the electron density. *Phys Rev B*, 1988; 37: 785.[DOI]

[26] Dunning Jr TH, Hay PJ. Modern Theoretical Chemistry. In: Schaefer HF (Eds); Plenum, New York, USA; 1976: 805.

[27] Mosmann T. Rapid colorimetric assay for cellular growth and survivals: Application to proliferation and cytotoxicity assays. *J Immunol Methods*, 1983; 65: 55-63.[DOI]

[28] Hernanz A, Billes F, Bratu I et al. Vibrational analysis and spectra of orotic acid. *Biopolym Orig Res Biomol*, 2000; 57: 187-198.[DOI]

[29] Wysokiński R, Morzyk-Ociepa B, Głowiak T et al. Revised molecular structure and vibrational spectra of tetraaqua (orotato) nickel (II) monohydrate: band assignment based on density functional calculations. *J Mol Struct (Theochem)*, 2002; 606: 241-251.[DOI]

[30] Baran EJ, Mercader RC, Hueso-Ureña F et al. Crystal structure, raman and 57Fe mo ssbauer spectra of the FeII complex of iso-orotic acid. *Polyhedron*, 1996; 15: 1717-1721.[DOI]

[31] Batt RD, Martin JK, Ploeser J Mc T et al. Chemistry of the di-hydropyrimidines. Ultraviolet spectra and alkaline decomposition. *J Am Chem Soc*, 1955; 76: 3665.[DOI]

[32] Icbudak H, Olmez H, Yesilel OZ et al. Syntheses, characterization and crystal structures of novel amine adducts of metal saccharinates, orotates and salicylates. *J Mol Struct*, 2003; 657: 255-270.[DOI]

[33] Papaefstathiou GS, Manessi S, Raptopoulou CP et al. The first metal complex of 5-hydroxyorotic acid: dimethylammonium bis (N, N-dimethylformamide) bis (5-hydroxyorotato (-2)) gallate (III). *Inorg Chem Comm*, 2004; 7: 69-72.[DOI]

[34] Kostova I, Peica N, Kiefer W. Theoretical and spectroscopic studies of new lanthanum (III) complex of orotic acid. *Vibr Spectrosc*, 2007; 44: 209-219.[DOI]

[35] Lencioni S, Pellerito A, Fiore T et al. Organometallic complexes with biological molecules. X: Dialkyltin (IV) and trialkyltin (IV) orotates: Spectroscopic and in vivo investigations. *Appl Organometal Chem*, 1999; 13: 145-157.[DOI]

[36] Exner K, Fischer G, Bahr N et al. Proximate, syn-Periplanar Bisdiazene Skeletons: Syntheses, Structures, Homoconjugate Reactivity and Photochemistry. *Eur J Org Chem*, 2000; 5: 763-785.[DOI]

[37] Castaneda J, Denisov GS, Kucherov SY et al. Infrared and ab initio studies of hydrogen bonding and proton transfer in the complexes formed by pyrazoles. *J Mol Struct*, 2003; 660: 25-40.[DOI]

[38] Gonzalez-Sanchez F. Infra-red spectra of the benzene carboxylic acids. *Spectrochim Acta*, 1958; 12: 17-33.[DOI]

[39] Hadzi D, Sheppard N. The infra-red absorption bands associated with the COOH and COOD groups in dimeric carboxylic acids. I. The region from 1500 to 500 cm^{-1}. *Proc Roy Soc Ser A*, 1953; 216: 247-266.[DOI]

[40] Lin-Vien D, Colthup NB, Fateley WG, Grasselli JG. The Handbook of Infrared and Raman Characteristic Frequencies of Organic Molecules. Academic Press Inc., San Diego, CA, USA; 1991: 140.

[41] Dolish FR, Fateley WG, Bentley FF. Characteristic Raman Frequencies of. Organic Compounds. John Wiley&Sons Inc., 1974: 128.

[42] Orza JM, García MV, Alkorta I et al. Vibrational spectra of 3,5-dimethylpyrazole and deuterated derivatives. *Spectrochim Acta A*, 2000, 56: 1469-1498.[DOI]

[43] Szabo A, Češljević VI, Kovács A. Tautomerism, hydrogen bonding and vibrational properties of 4-acetyl-3(5)-amino-5(3)-methylpyrazole. *Chem Phys*, 2001; 270: 67-78.[DOI]

[44] Sourisseau C, Fouassier M, Mauricot R et al. Structure and bonding in cerium oxysulfide compounds. II—Comparative lattice dynamics calculations on Ce_2O_2S and $Ce_{2.0}O_{2.5}S$. *J Raman Spectrosc*, 1997; 28: 973-978.[DOI]

[45] Lu Y, Deng G, Miao F et al. Metal ion interactions with sugars. The crystal structure and FT-IR study of the $NdCl_3$–ribose complex. *Carbohydrate Res*, 2003; 338: 2913-2919.[DOI]

[46] Sohn JR, Chun EW, Pae YI. Spectroscopic studies on ZrO_2 odified with MoO_3 and activity for acid catalysis. *Bull Korean Chem Soc*, 2003; 24: 1785-1792.[DOI]

[47] Jayaraman A, Sharma SK, Wang SY et al. Pressure-induced phase transitions in KDy(MoO4)2 and KY(MoO4)2: A high-pressure Raman study. *J Raman Spectrosc*, 1996; 27: 485-490.[DOI]

[48] Fielicke A, Meijer G, Von Helden G. Infrared multiple photon dissociation spectroscopy of transition metal oxide cluster cations. *Eur Phys J D*, 2003; 24: 69-72.[DOI]

[49] Lewandowski W, Dasiewicz B, Koczon P et al. Vibrational study of alkaline metal nicotinates, benzoates and salicylates. *J Mol Struct*, 2002; 604: 189-193.[DOI]

[50] Koczon P, Lewandowski W, Mazurek AP. Vibrational (FT-IR and FT-Raman) and NMR studies on selected metal (Ca, Mn, Zn) complexes with ortho-, meta-, and para-iodobenzoic acids. *Vibr Spectrosc*, 1999; 20: 143-149.[DOI]

[51] Kakiuchi M, Abe T, Nakayama H. D/H fractionation factor between water vapor and crystal water of copper chloride dihydrate: Statistical mechanical approach based on Raman spectra. *Geochem J*, 2001; 35: 285-293.[DOI]

[52] Wang K, Li YS. Silver doping of polycarbonate films for surface-enhanced Raman scattering. *Vibr Spectrosc*, 1997; 14: 183-188.[DOI]

[53] Boerio FJ, Hong PP, Clark PJ et al. Surface-enhanced Raman scattering from model acrylic adhesive systems. *Langmuir*, 1990; 6: 721-727.[DOI]

[54] Kwon YJ, Son DH, Ahn SJ et al. Vibrational spectroscopic investigation of benzoic acid adsorbed on silver. *J Phys Chem*, 1994; 98: 8481-8487.[DOI]

[55] Galdecka E, Galdecki Z, Huskowska E et al. Crystal structure and optical properties of Ln(III) octahedral complexes with hexamethylphosphortriamide; $[Ln(HMPA)_6](ClO_4)_3$. *J Alloys Compd*, 1997; 257: 182-190.[DOI]

[56] de Andrés A, Taboada S, Martínez JL et al. Optical phonons in R_2BaMO_5 oxides with M=Co, Ni, Cu, and R=a rare earth. *Phys Rev B*, 1993; 47: 14898-14904.[DOI]

[57] Cho BO, Lao SX, Chang JP. Origin and effect of impurity incorporation in plasma-enhanced ZrO2 deposition. *J Appl Phys*, 2003; 93: 9345-9351.[DOI]